Targeting Helicobacter pylori urease activity and maturation: In-cell high-throughput approach for drug discovery

# Targeting *Helicobacter pylori* urease activity and maturation: in-cell high-throughput approach for drug discovery

Cinzia Tarsia[#], Alberto Danielli[#], Francesca Florini, Paolo Cinelli, Stefano Ciurli, Barbara Zambelli*

Department of Pharmacy and Biotechnology, University of Bologna, Viale G. Fanin 40, 40127 Bologna (Italy)

*barbara.zambelli@unibo.it

[#]CT and AD contributed equally to this work

**Abstract**

**Background**. *Helicobacter pylori* is a bacterium strongly associated with gastric cancer. It thrives in the acidic environment of the gastric niche of large portions of the human population using a unique adaptive mechanism that involves the catalytic activity of the nickel-dependent enzyme urease. Targeting urease represents a key strategy for drug design and *H. pylori* eradication.

**Method**. Here, we describe a novel method to screen, directly in the cellular environment, urease inhibitors. A ureolytic *Escherichia coli* strain was engineered by cloning the entire urease operon in an expression plasmid and used to test in-cell urease inhibition with a high-throughput colorimetric assay. A two-plasmid system was further developed to evaluate the ability of small peptides to block the protein interactions that lead to urease maturation.

**Results**. The developed assay is a robust cellular model to test, directly in the cell environment, urease inhibitors. The efficacy of a co-expressed peptide to affect the interaction between UreF and UreD, two accessory proteins necessary for urease activation, was observed. This event involves a process that occurs through folding upon binding, pointing to the importance of intrinsically disordered hot spots in protein interfaces.

**Conclusions**. The developed system allows the concomitant screening of a large number of drug candidates that interfere with the urease activity both at the level of the enzyme catalysis and maturation.

**General significance.** As inhibition of urease has the potential of being a global antibacterial strategy for a large number of infections, this work paves the way for the development of new candidates for antibacterial drugs.

**Keywords**: urease; nickel delivery; drug screening; protein-protein interactions; enzyme inhibitors; *Helicobacter pylori*

## 1. Introduction

*Helicobacter pylori* is a widespread Gram-negative bacterium infecting the stomach of millions of people every year, up to 50 % of adults and reaching 80 – 90 % in developing countries [1]. After colonization, untreated *H. pylori* infections persist, often asymptomatically, for the entire life-span of the host, because of the inability of the human immune response to efficiently counteract the bacterium. The infection causes chronic inflammation of the gastric mucosa, which can slowly progress to gastric adenocarcinoma or mucosa-associated lymphoid tissue (MALT) lymphoma. Accordingly, in 1994 the WHO classified *H. pylori*, first and unique among all bacteria, as a class I carcinogen [2] and reconfirmed this classification in 2012 [3]. Several meta-analyses pointed out that eradication of *H. pylori* at the population level would have beneficial effects, such as reduction in gastric cancer incidence, peptic ulcer development, dyspepsia symptoms, and anemia occurrence[4]. In addition, *H. pylori* eradication causes complete regression in 60%-80% of already established MALT lymphomas [5]. Therefore, the Gastric Cancer Consensus Conference boldly recommended population-based screening and treatment for *H. pylori* to prevent gastric cancer [6].

Nonetheless, treatment efficacy remains a major concern. The standard first-line therapy to eradicate *H. pylori*, using a combination of three different antibiotics, fails in 20% of the cases because of antibiotic resistance, leading to an increasing number of infected individuals harboring resistant bacteria. Indeed, in 2017 WHO included *H. pylori* in the list of antibiotic-resistant bacteria for which antibiotic development is a global priority [7].

To survive inside the very acidic environment of the gastric niche, *H. pylori* has created a unique adaptive mechanism relying on the Ni(II)-dependent enzyme urease, which catalyzes the rapid hydrolysis of urea to produce ammonia and carbamate. The latter spontaneously hydrolyzes, generating an increase of pH that buffers the micro-environment surrounding the

bacterium [8,9]. Indeed, urease-deficient *H. pylori* strains cannot colonize the stomach niche of mice [10]. Similarly, mutants that can synthesize the apo-urease but are unable to incorporate Ni(II) into its active site are unable to colonize the gastric mucosa, thereby highlighting a link between Ni(II) activation of urease and host colonization [11]. Interestingly, standard therapy reaches significantly higher eradication rates if a nickel-free diet is maintained by infected patients, suggesting that the reduction of urease activity could increase the bacterial susceptibility to antibiotics [12]. Higher eukaryotes do not produce urease, nor other nickel enzymes, rendering urease activity an attractive target for the development of alternative and specific antibacterial strategies to overcome *H. pylori* gastric infection.

Urease proteins are generally heteropolymeric proteins with a quaternary structure $(\alpha\beta\gamma)_3$[8]. In bacteria of the genus *Helicobacter* the trimer is of the type $(\alpha\beta)_3$, with the $\beta$ subunits corresponding to the fused $\beta$ and $\gamma$ subunits normally found in other bacteria. The protein also presents a higher level of oligomerization, with an $[(\alpha\beta)_3]_4$ quaternary structure. The activity of urease relies on the presence of a binuclear active site containing two Ni(II) ions, bridged by the carboxylate group of a carbamylated lysine, essential to maintain the ions at the right distance for the catalysis, and by a hydroxide ion, the nucleophile of the hydrolysis reaction [8,13]. This architecture, always present in the $\alpha$ subunit, is fully conserved in all known urease structures. Nickel incorporation into the active site of urease occurs post-translationally during enzyme maturation, and requires the assistance of the accessory proteins UreD, UreF, UreG and UreE, expressed from genes belonging to the urease operon [14]. UreE is a homodimeric protein responsible for Ni(II) delivery into the urease active site, while UreG is an intrinsically disordered GTPase that energizes the process of urease maturation [15]. In solution, UreE and UreG form a complex $UreE_2$-$UreG_2$, whose structure

has been obtained with molecular modeling and protein docking [16], and subsequently confirmed by NMR [14]. The crystal structure of $UreD_2$-$UreF_2$-$UreG_2$ was reported [17], this larger complex being a multiprotein composite chaperone that pre-activates apo-urease before Ni(II) incorporation, a modification necessary for the enzyme to build up a correct active site.

In an attempt to provide a model system to test new antibacterial molecules that target *H. pylori*, we engineered a ureolytic *E. coli* strain to screen urease inhibitors by means of an in-cell high-throughput colorimetric assay. In addition, we set up a two-plasmid system to evaluate the ability of peptide sequences to block the protein-protein interactions (PPIs) among the accessory proteins that lead to enzyme maturation. This method was used successfully to screen the inhibition activity of a co-expressed peptide.

## 2. Experimental section

### 2.1. Gene cloning and site-directed mutagenesis

A scheme of the cloning strategy used in this work is presented in Figure 1SI. A list of the plasmids used in this work, with a short description, and of the oligonucleotide sequences needed for the molecular biology setup is reported in Table SI1 and SI2 respectively. Briefly, the *pGEM-ureOP* plasmid, carrying the *H. pylori* strain G27 urease operon (National Center for Biotechnology Information code NC_011333.1) [18], was used as PCR template for amplifying the *ureABIE* portion of the urease operon, containing the structural urease genes *ureA* and *ureB*, the urea membrane transporter gene *ureI* and the metallo-chaperone gene *ureE*, using ureOP_F and ureE_R. The purified PCR product was ligated (T4 DNA ligase) into the *pGEM-T* Easy vector according to the manufacturer instructions. The resulting construct (*pGEM-ureABIE*) was purified, analyzed by restriction analysis, and sequenced at the 5' and 3' ends to verify the correct insertion of the partial operon. Site directed mutagenesis was performed on *pGEM-ureOP* to create a urease operon containing a truncated version of *ureF* gene, lacking the C-terminal 21 residues (here called *pGEM-ureOP*$\Delta\alpha$F), by amplifying the entire plasmid using the mutagenic primers ureF_STOP and ureF_Blg_R. Using *pGEM-ureOP* as a template, *ureF* gene was amplified using ureF_Xho_F and ureF_Hind_R oligos. The gene was double-digested using XhoI and HindIII restriction enzymes and eventually cloned into the *pBAD/His-Myc* vector (ThermoFisher) digested with the same restriction enzymes. This construct was used as template for amplifying the *araC-pBAD-ureF* portion, containing the *ureF* gene downstream to the arabinose promoter, using the pBAD_XbaI_F and pBAD_BspHI_R oligonucleotides. Similarly, the *pXG-0* vector [19] was used as a template for a PCR reaction using HSC_Xba_F and HSC_BspH_R oligonucleotides, generating a DNA fragment containing the pSC101 origin of replication and the

chloramphenicol resistance gene. The *pBAD-ureF* and *pXG-0* PCR products were double-digested using XbaI and BspHI and ligated to give the *pXG0-pBAD-ureF* construct, containing the *ureF* gene under the control of the arabinose promoter, and with the pSC101 origin of replication and the chloramphenicol acetyl transferase gene. This construct was then digested using XhoI and HindIII restriction enzymes and the gene coding for the 21-residues C-terminal α-helix of UreF (αF), obtained by annealing the αF_Xho_F and αF_Hind_R oligos was cloned in under the control of arabinose promoter.

Finally, the αF coding gene, deriving from the annealing of αF_Nco_F and αF_Bam_R oligos was cloned in frame with the GB1 gene in the *pETM-12* [20] previously digested with NcoI and BamHI. Subsequently, the *GB1-αF* gene was amplified using the GB1αF-Xho_F and GB1αF-Hind_R, double digested with XhoI and HindIII and cloned into the *pXG0-pBAD* vector, to obtain *pXG0-pBAD*-GB1αF plasmid expressing GB1 protein fused with αF.

**2.2. In-cell urease activity test**

TOP10 cells harboring *pGEM-ureOP* plasmid or its derivatives, co-transformed, if needed, with *pXG0-pBAD-ureF*, *pXG0-pBAD-αF* or *pXG0-pBAD-GB1αF* were pre-cultured at 37 °C in 1 mL of lysogeny broth (LB) containing 50 µg/mL of carbenicillin (Cb), and, for the double transformant, 25 µg/mL of chloramphenicol (Cm). After 16 hours, 200 µL were used to inoculate 2 mL of M9 medium (1 liter contained 6 g of $Na_2HPO_4$, 3 g of $KH_2PO_4$, 0.5 g of NaCl, 1.25 g of $(NH_4)_2SO_4$, 0.246 g of $MgSO_4$, 4 g of glucose) containing the appropriate antibiotics and 10 µg/L of cresol red pH indicator. When OD600 reached 0.7-0.9, 100 µL of each culture were inoculated in 96-well plates with the appropriate concentration of urea, and with or without 0.5% arabinose or the appropriate inhibitor concentrations. Immediately before running the experiment, $NiSO_4$ was added to each culture. In each well, 50 µL of mineral oil

were added to prevent medium evaporation during the culture. The color change of cresol red indicator was monitored over time spectrophotometrically in a multi-plate reader, measuring the absorption at 430 nm and at 580 nm.

## 3. Results

### 3.1. In-cell test of urease activity

The 6,500 bp urease operon[8] (*ureOP*) coding for both the structural and accessory genes of the *Helicobacter pylori* enzyme (Figure 1A) was cloned in an expression vector to yield *pGEM-ureOP* (Figure 1B and Figure 1SI) and used to express the holo-urease enzyme in recombinant BL21(DE3) *E. coli*, as previously described [18].

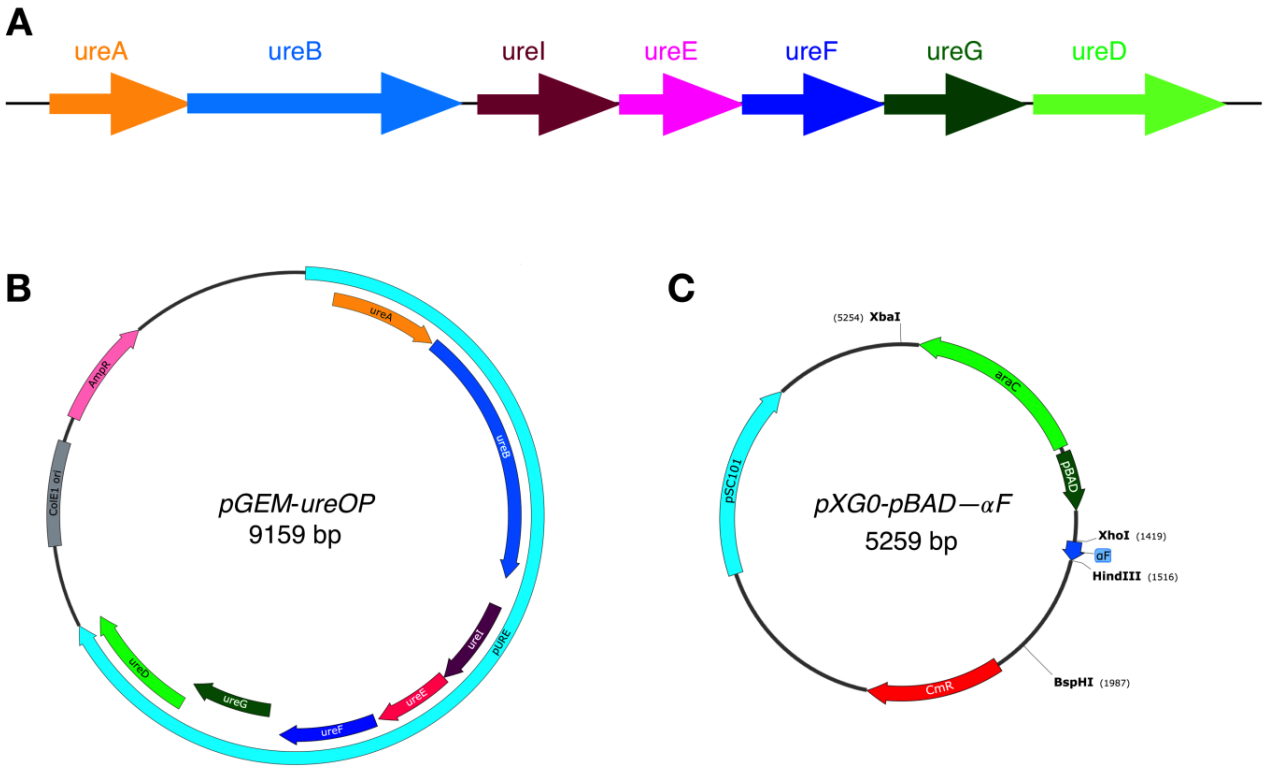


**Figure 1.** (**A**) *H. pylori* urease operon, cloned in a *pGEM-T*-Easy vector to yield *pGEM-ureOP* (**B**). The complementing plasmid, expressing αF under the expression control of arabinose promoter, is represented in (**C**).

To evaluate the urease activity in the cytoplasm of growing bacteria, the same genetic construct was used to transform Top10 *E. coli* cells. The recombinant bacteria maintained urease expression and activity, driven by the vector-encoded *lac* promoter upstream of the

*ure* operon. In addition, the *recA*- genotype of this strain ensured higher stability of the genetic constructs, preventing unwanted recombination, especially when two plasmids harboring similar sequences were co-transformed, a condition required for the experiments described below.

The pH increase of the bacterial environment catalyzed by urease was used as a detection system to evaluate the ureolytic capacity of the engineered *E. coli* strain, modifying a previously reported protocol [21]. Indeed, the faster the urea hydrolysis, the more rapid and distinct the increase of pH of the medium, resulting in a turning of a pH indicator, measured as a change of absorbance whose slope is directly proportional to reaction rate. To find the optimal assay conditions, the experiment was performed with different substrate and Ni(II) concentrations (50 to 500 mM urea, Figure 2A; 0 to 750 μM Ni(II), Figure 3), added to the medium when cells reached the exponential growth. The dependence of the initial rate of reaction on urea concentration (Figure 2B) decreases at substrate concentrations of 300 mM urea, which is close to the maximal velocity of reaction ($v_{max}$) reached at 500 mM urea. These data cannot be fit using a Michaelis-Menten treatment, possibly because other events, such as urea penetration through the plasma membrane, influence the kinetics of the substrate availability, and consequently affect the overall enzymatic reaction kinetics. It is interesting to note that the $K_M$ measured for urea hydrolysis by *H. pylori* urease is 0.17 mM or 0.79 mM [22] *in vitro*, suggesting that only a minor fraction of urea is able to reach the cytoplasmatic environment. Alternatively, this can be due to differences in the reaction conditions, such as different pH, ionic strength, presence of competing molecules in the bacterial media, used herein with respect to previous experiments carried out in vitro with purified urease.

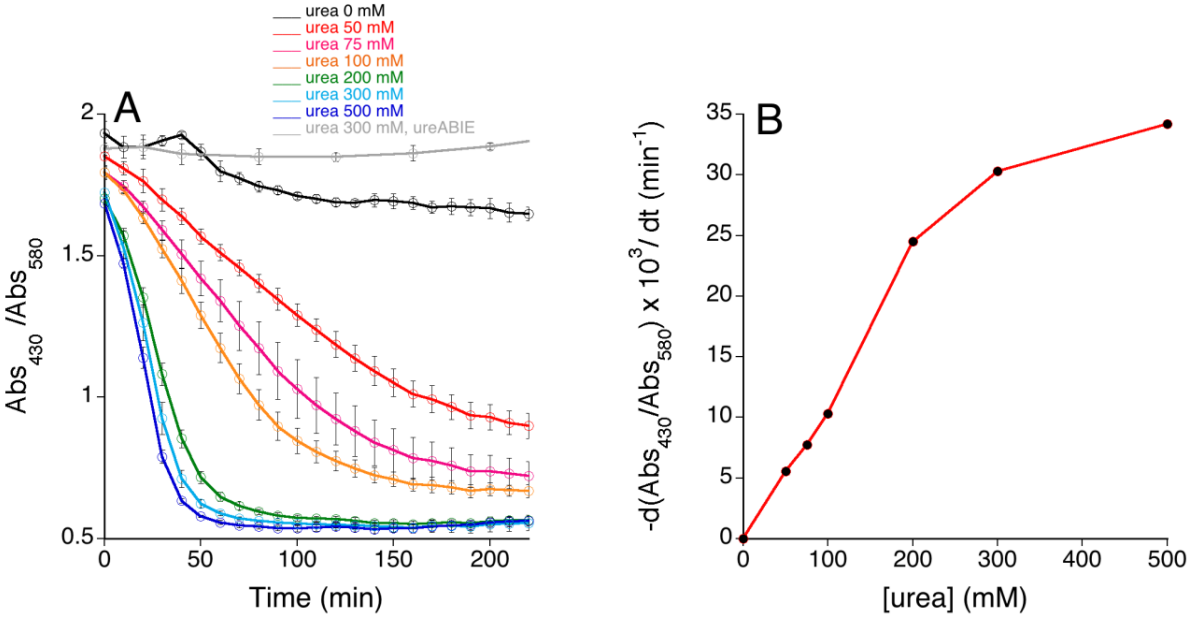


**Figure 2.** (**A)** Urease activity, measured as the ratio of absorbance at 430 nm and at 580 nm for the cresol red indicator, added to the *E. coli* culture harboring the *pGEM-ureOP* plasmid. The measures were performed in a 96-wells multiplate, after the addition of 250 µM Ni(II) and different concentrations of urea, as indicated. The urease activity of an inactive strain, *ureABIE*, transformed with a defective urease operon lacking most urease accessory genes, is also shown for comparison. Every measure was performed in triplicate and the error bars represent the standard deviations of the average values. (**B)** Initial velocity of urea hydrolysis at different urea concentrations, measured as the slope of the first four points of the curves shown in (A).

The dependence of urease activity on Ni(II) concentration was tested both with substrate concentrations corresponding to a rate lower than half of $v_{max}$ (75 mM, Figure 3A) and close to $v_{max}$ (300 mM, Figure 3B). Under both conditions, no significant variation of hydrolysis rates was observed between 250 µM and 750 µM Ni(II), and therefore 250 µM was the metal concentration added in all subsequent assays.

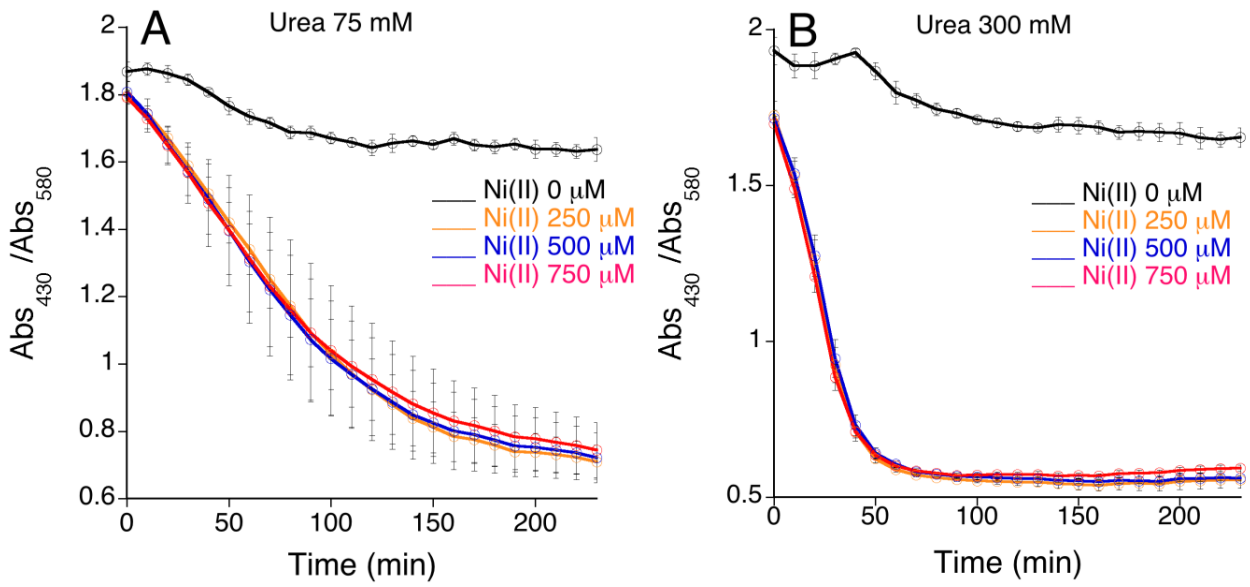


**Figure 3.** Urease activity, measured as the ratio of absorbance at 430 nm and at 580 nm for the cresol red indicator, added to the *E. coli* culture harboring the *pGEM-ureOP* plasmid. The measures were performed in a 96-wells multiplate, after the addition of different Ni(II) concentrations, as indicated, and of either 75 mM (**A**) or 300 mM (**B**) urea. Every measure was performed in triplicate and the error bars represent the standard deviations of the average values.

### 3.2. In-cell urease inhibition

To test the ability of known urease inhibitors to exert their action on the over-expressed enzyme in growing bacteria, these compounds were added at variable concentrations to the growth medium of *E. coli*, and the urease activity was measured as previously described. All inhibition assays were conducted at substrate concentration corresponding both to $v_{max}$ (300 mM urea) and to a rate lower than half of $v_{max}$ (75 mM urea) to evaluate the competitive nature of urease inhibition. Cultures that did not include the pH indicator were run in parallel to monitor the bacterial growth following the optical density at 600 nm, in order to exclude the toxicity of the tested molecules. In addition, equal dilutions of *E. coli* cultures, containing the highest inhibitor concentrations used, were plated at the end of each experiment and the number of colony forming units was compared with the ones generated in the absence of urease inhibitors. No significant variation in cell viability was observed for cells grown in the

presence of the selected compounds.

*3.2.1. Fluoride and borate*

Fluoride has been reported to exert a mixed inhibition with a predominance of an uncompetitive mechanism[23]. While the uncompetitive inhibition constant remains substantially stable in the pH range from 6.5 ($K_{iuc(F-)}$ = 0.28 mM) and 8 ($K_{iuc(F-)}$ = 0.43 mM) for *Sporosarcina pasteurii* urease, the contribution of competitive inhibition is significant at pH 6.5 ($K_{ic(F-)}$ = 0.79 mM) and becomes negligible at pH 8[23]. The double mode of inhibition is related to two fluoride ions bound to the enzyme active site: the first one, responsible for the competitive inhibition, substitutes the substrate urea binding one of the two Ni(II) ions in the active site, while the second one, involved in the uncompetitive inhibition, binds in place of the nucleophilic hydroxide [23].

Differently, boric acid shows competitive inhibition in the form $B(OH)_3$, binding as a substrate analogue to the enzyme active site and leaving in place the nucleophilic hydroxide[24]. Inhibition constants $K_{i(B(OH)3}$ = 0.099 mM and 0.34 mM were reported for bacteria such as *Proteus mirabilis* and *Klebsiella aerogenes* respectively[25].

Consistently with the inhibition constants measured *in vitro*, in-cell assays were conducted with fluoride and borate concentrations between 0.5 mM and 5 mM, at 75 mM and 300 mM urea concentrations (Figure 4). For both fluoride (Figure 4A) and borate (Figure 4B), the inhibition effect resulted negligible, suggesting that these compounds are not able to efficiently cross the plasma membrane of the Gram-negative *E. coli*. This observation proves that the observed urease activity is ascribed to the cytoplasmatic urease, while the amount of active enzyme in the extracellular medium is negligible.

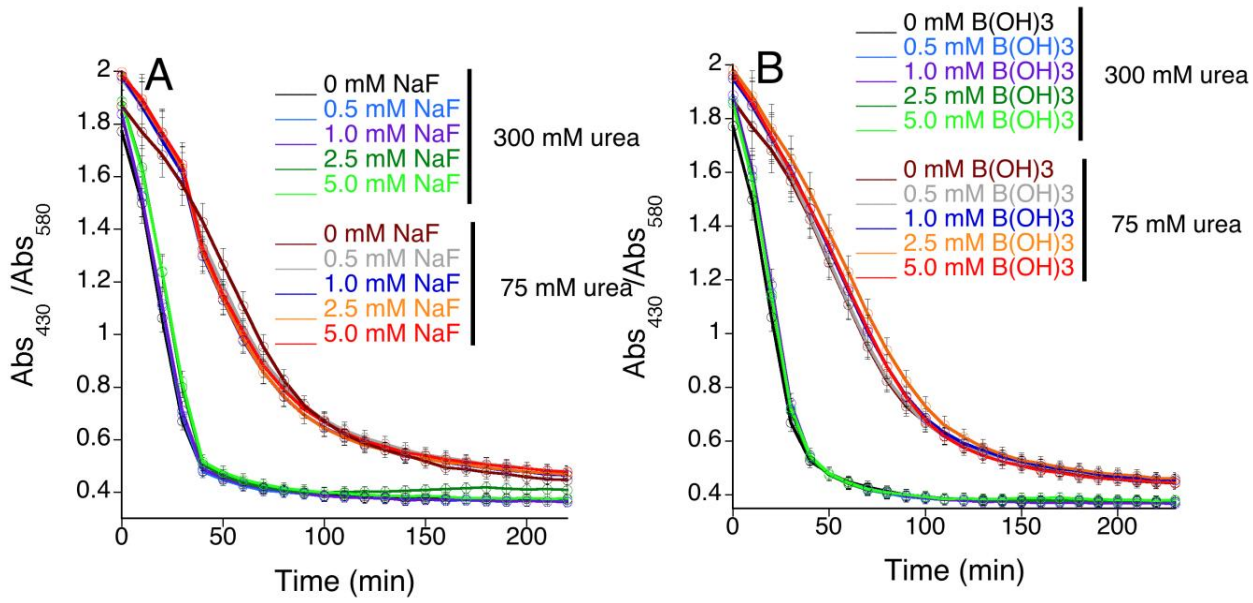


**Figure 4.** Urease activity, measured as the ratio of absorbance at 430 nm and at 580 nm for the cresol red indicator, added to the *E. coli* culture harboring the *pGEM-ureOP* plasmid, in the presence of increasing concentrations of fluoride (**A**) or boric acid (**B**) urease inhibitors. The measures were performed in a 96-wells multiplate, after the addition of 250 μM Ni(II) and of 75 mM and 300 mM urea. Every measure was performed in triplicate. The error bars represent the standard deviations of the average values.

### *3.2.2. AHA and NBPT*

Aceto-hydroxamic acid (AHA) and N-(n-butyl)-thiophosphoric triamide (NBPT) are well-known competitive, slow binding, urease inhibitors. AHA binds the urease active site with the hydroxamate oxygen atom bridging the two Ni(II) ions, while the carbonyl oxygen chelates one Ni(II) ion.[26–28] This compound shows a bactericidal effect on *H. pylori*,[29] and is the only urease inhibitor used in therapy to treat urinary tract infections[30], despite its severe side effects such as teratogenicity and toxicity[31]. The *in vitro* inhibition constant for *H. pylori* urease is $K_{i(AHA)}$ = 2 μM [32]. In this in-cell assay, high concentrations (1 mM) of AHA added to the medium show a partial reduction of urease activity only at lower urea concentrations, supporting the competitive nature of AHA inhibition observed *in vitro* (Figure 5). An $IC_{50}$ = 1.1 mM can be derived by the data at 75 mM urea, similar to the $IC_{50}$ measured for *H. pylori* J99

strain, reported between 1.35 mM and 1.66 mM [33]. The high AHA concentrations needed to obtain urease inhibition suggest the partial absorption of AHA by the *E. coli* membrane, and provides a rationale for the large doses (~ 1000 mg/day for adults) required for its administration *in vivo* [34].

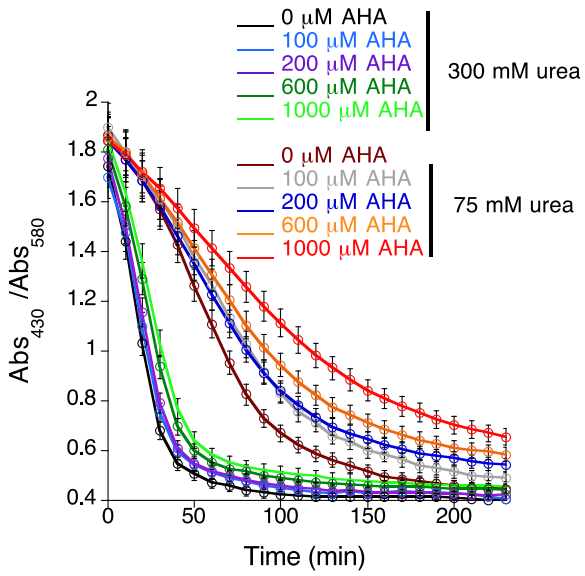


**Figure 5.** Urease activity, measured as the ratio of absorbance at 430 nm and at 580 nm for the cresol red indicator, added to the *E. coli* culture harboring the *pGEM-ureOP* plasmid, in the presence of increasing concentrations of AHA inhibitor, as indicated. The measures were performed in a 96-wells multiplate, after the addition of 250 μM Ni(II) and of 75 mM and 300 mM urea. Every measure was performed in triplicate. The error bars represent the standard deviations of the average values.

On the other hand, NBPT interacts with urease after an initial hydrolytic event that forms the mono-deaminated form (NBPD), which is further hydrolyzed in the presence of urease forming monoamine thiophosphate (MATP); the latter thus coordinates the Ni(II) ions in the active site of the enzyme [35]. The NBPT competitive inhibition constant is $K_{ic(NBPT)}$ 6.4 μM for *S. pasteurii* urease and 0.94 μM for jack bean urease [35]. In bacterial cultures, NBPT was active both at lower (Figure 6A) and at higher (Figure 6B) urea concentrations, showing an $IC_{50}$ of 23 μM and 31 μM respectively. The lower value for $IC_{50}$ obtained at low urea concentrations is consistent with its competitive inhibition mechanism.

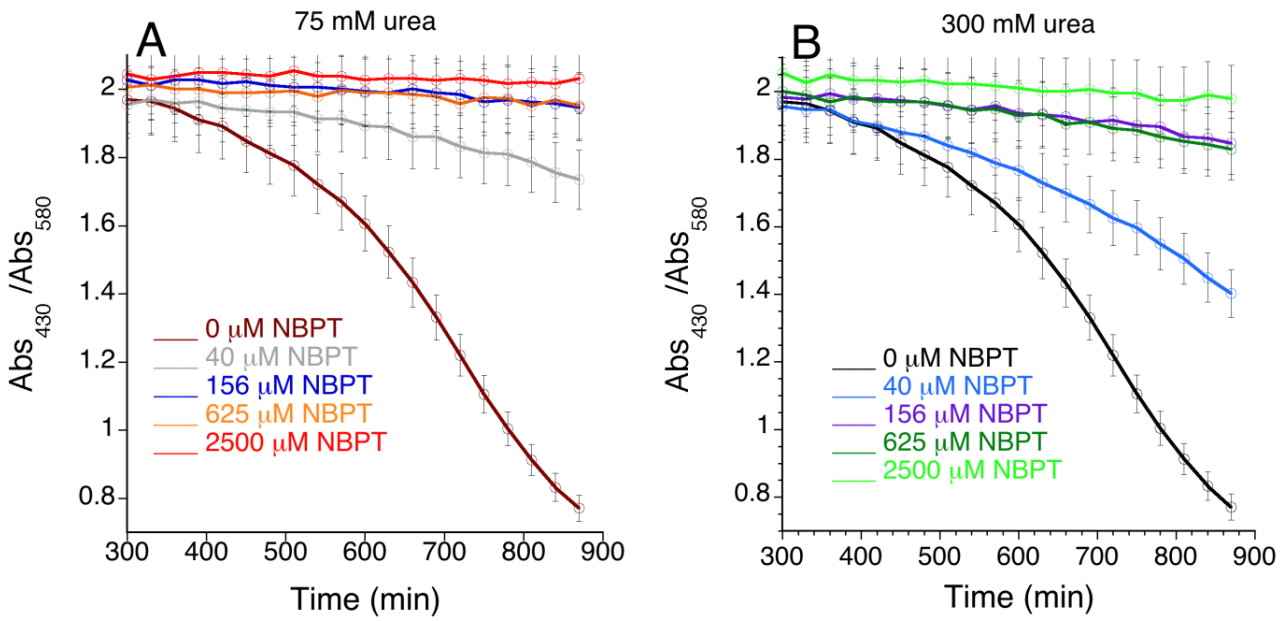


**Figure 6.** Urease activity, measured as the ratio of absorbance at 430 nm and at 580 nm for the cresol red indicator, added to the *E. coli* culture harboring the *pGEM-ureOP* plasmid, in the presence of increasing concentrations of NBPT inhibitor. The measures were performed in a 96-wells multiplate, after the addition of 250 μM Ni(II) and of 75 mM (**A**) and 300 mM (**B**) urea. Every measure was performed in triplicate. The error bars represent the standard deviations of the average values.

### *3.2.3. 1,4-benzoquinone*

A distinctive inhibition mechanism is observed in the case of quinones. These compounds easily react with thiols to give the thiol-substituted benzene-1,4-diol. In particular, the crystal structure of urease inhibited by 1,4-benzoquinone (BQ) indicates that this compounds targets the conserved Cys residue present in the flap regulating the access to the active site pocket[36]. Covalent modifications of this residue lead to enzyme inactivation. This is consistent with the observed process of uncompetitive enzyme inhibition, with a kinetic constant $k$ = 1.24 ± 0.06 × $10^3$ $M^{-1}$ $s^{-1}$ [36]. The minimum concentration of BQ required to observe this effect *in vitro* is 18 μM [36]. In-cell, BQ shows an inhibitory effect both at lower (Figure 7A) and higher (Figure 7B) substrate concentrations, with a calculated $IC_{50}$ of 55 μM in both conditions. This observation confirms, *in vivo,* the uncompetitive nature of the

inhibition reported *in vitro*. The concentration range of BQ effect is comparable in cell and *in vitro*, suggesting that this compound is able to efficiently move through the Gram-negative plasma membrane.

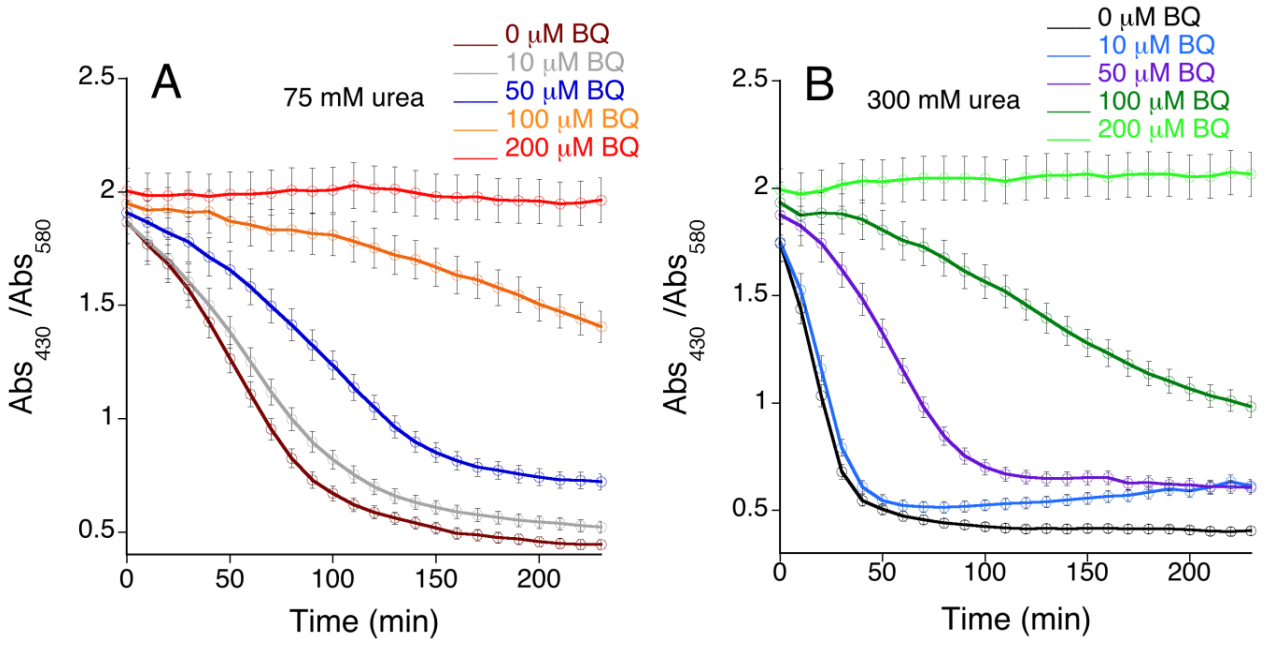


**Figure 7.** Urease activity, measured as the ratio of absorbance at 430 nm and at 580 nm for the cresol red indicator, added to the *E. coli* culture harboring the *pGEM-ureOP* plasmid, in the presence of increasing concentrations of benzoquinone inhibitor. The measures were performed in a 96-wells multiplate, after the addition of 250 μM Ni(II) and of either 75 mM (**A**) or 300 mM (**B**) urea. Every measure was performed in triplicate. The error bars represent the standard deviations of the average values.

### 3.3. In-cell inhibition of urease maturation

A possible alternative route to inhibit urease activity is to prevent the construction of the active site that requires Ni(II) ions insertion, targeting the protein-protein interactions (PPIs) between the chaperones that carry out urease maturation. To identify the interaction "hot spots", that is the protein segments that contribute most significantly to the binding interface indicative for the most promising "druggable" interfaces, the Peptiderive protocol [37] (http://rosie.rosettacommons.org/peptiderive) was applied, starting from the crystal structure of the $UreF_2$-$UreD_2$ heterodimer [38] (Figure 8A). When UreD was assigned as the receptor

for the peptide, and a query for a sequence of 10 and 20 residues was submitted for the inhibitor peptide, the protocol detected a hot spot region at the C-termini of the UreF sequence (D$^{226}$ESHLCTA**SVQNDIKAMQ**HE$^{245}$ for the 20 residue segment, the 10 residue segment is represented in bold), including an $\alpha$-helical motif (underlined) that, in the crystal structure, makes extended contacts with UreD (Figure 8A) [38]. This sequence is located in a protein region that is degraded from Ser$^{234}$ due to disorder when UreF is expressed in the absence of its partner[39], therefore suggesting that the PPI is stable enough to protect this part from proteolytic cleavage. This observation also implies that this interaction involves a disorder-to-order transition. To confirm the role of this sequence in the PPI, we mutated the *ureF* gene found in the *pGEM-ureOP* genetic construct, introducing a stop codon at position 233 to delete the region (here called $\alpha$F) containing the C-terminal 21 residues of the protein. The recombinant strain produced a urease-inactive culture, proving that this protein segment is essential for the formation of an active $UreF_2$-$UreD_2$ complex and consequent urease activation in the bacteria (Figure 8B, light blue curve). A similar urease-negative phenotype was observed with *E. coli* transformed with *pGEM-ureABIE* vector, which lacks the accessory genes *ureF*, *ureD* and *ureG* genes (Figure 8B, orange curve).

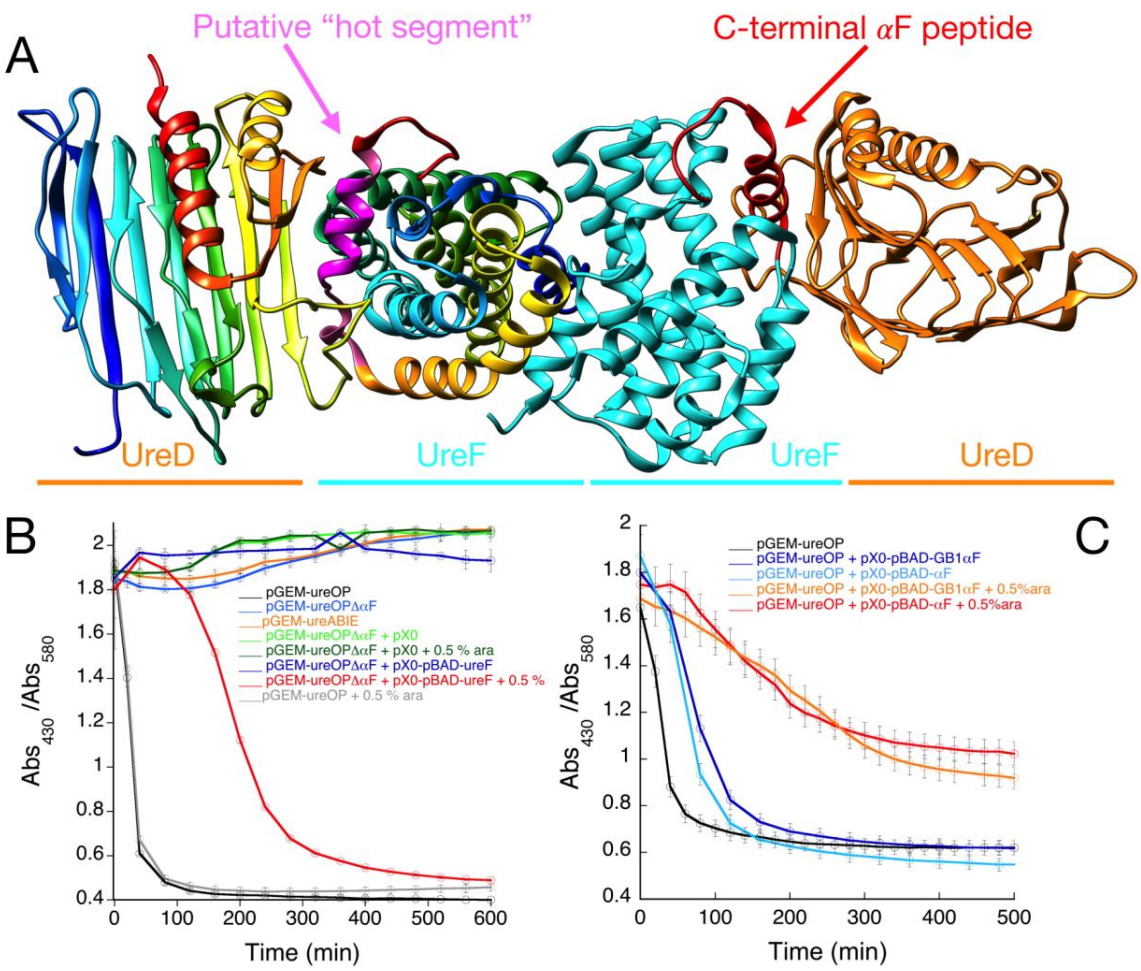


**Figure 8.** (**A**) Crystal structure of the $UreD_2$-$UreF_2$ complex (PDB code: *3SF5*). For each protein, a chain is represented coloring successive residues from blue (N-terminus) to red (C-terminus). The second chain is colored in cyan (UreF) or in orange (UreD). The C-terminal segment of UreF (αF, in magenta) is sensitive to proteolysis and is preserved only upon the PPI. The "hot segments" found by Peptiderive are depicted in pink (20-residue segment) and in magenta (10-residue segment). (**B**) Urease activity, measured as the ratio of absorbance at 430 nm and at 580 nm for the cresol red indicator, added to the *E. coli* culture harboring *pGEM-ureOP*, either in the wild type or the mutated versions, both alone or complemented with empty *pXG0* or *pXG0-pBAD-ureF* plasmids. When indicated, 0.5 % arabinose inducer was added to the bacterial culture. The measures were performed in a 96-wells multiplate, after the addition of 250 µM Ni(II) and 300 mM urea. Every measure was performed in triplicate and the error bars represent the standard deviations of the average values. (**C**) Urease activity, measured as the ratio of absorbance at 430 nm and at 580 nm for the cresol red indicator added to the *E. coli* culture harboring wild-type *pGEM-ureOP* alone or co-transformed with *pXG0-pBAD-GB1*-αF or *pXG0-pBAD*-αF plasmids. When indicated, 0.5 % arabinose inducer was added to the bacterial culture. The measures were performed in a 96-wells multiplate, after the addition of 250 µM Ni(II) and 300 mM urea. Every measure was performed in triplicate and the error bars represent the standard deviations of the average values.

A second plasmid carrying a copy of the wild-type *ureF* gene under the control of the arabinose promoter (*pBAD*) and with an origin of replication compatible with the *pGEM-ureOP* plasmid was produced (Figure 1C and SI1) and this construct, named *pXG0-pBAD-ureF*, was able to complement the mutation in a co-transformed strain only in the presence of arabinose inducer (Figure 8B, red curve). No complementation was observed in the absence of arabinose (Figure 8B, blue curve) or when the co-transformed plasmid did not contain the *ureF* gene (Figure 8B, light green and green curves).

This two-plasmid system was then used to prove the ability of the αF peptide to inhibit, after induction, in-cell urease activity. Arabinose-induced co-expression of the peptide (sequence MGSGSGSSVQNDIKAMQHESLYSRLYMS, UreF sequence underlined), alone (Figure 8C, red line) or fused to the C-terminus of the small globular protein GB1 [40] (Figure 8C, orange line), sensibly decreased the in-cell urease activity as compared to bacteria expressing the wild-type operon (Figure 8C, black line) or to the co-transformed bacteria in the absence of arabinose induction (Figure 8C, blue and light blue lines). Therefore, the identified sequence represents a leading interfering peptide to inhibit the urease activating PPIs.

## 4. Discussion

Urease is an essential virulence factor for *H. pylori* colonization of the human stomach and represents an attractive target for the development of antimicrobial strategies to counteract the increasingly emergent problem of antimicrobial resistance of this bacterium. Urease inactivation might be accomplished i) by designing specific enzyme inhibitors that selectively bind the active site of urease, preventing substrate binding and catalysis, or ii) by interrupting the protein-protein interaction (PPI) network that leads to Ni(II) delivery into the active site, precluding enzyme maturation. The first approach has been thoroughly pursued by searching for urease inhibitors that directly bind the Ni(II) ions in the active site or interfere with the catalytic cycle. Nevertheless, despite the large number of known urease inhibitors, this potential therapeutic route showed very limited success to date, with only few compounds evaluated in therapeutic studies presenting efficiency and safety concerns for their use *in vivo* [41]. Indeed, many drugs are not effective in therapy, or require very high dosage because of their low stability or limited bioavailability, not being able to efficiently diffuse inside the Gram-negative plasma membrane of the bacterium to reach their target in the cytoplasm. In this work, we addressed this problem by developing and optimizing a novel high-throughput screening system that allows to determine the capability of urease inhibitors directly in a physiological cell environment. In the past, the activity of urease was measured in the soluble fraction of the cellular extract after cellular lysis[18], and in batch measurements on whole *E. coli* cells resuspended in phosphate-buffered saline (PBS) buffer, incubated with urea and tested for urease activity at different time points [42]. Here, we took advantage of an ureolytic *E. coli* model system, obtained by transforming a commercial bacterial strain with a previously engineered plasmid expressing the urease operon (Figure 1)[18]. Bacterial cultures were then

grown in a 96-well plate and the in-cell urease activity was measured over time during cell growth at diverse concentrations of urea and Ni(II), applying a well-established pH-dependent colorimetric assay (Figure 2 and 3). Subsequently, the optimized assay conditions were used to test different types and concentrations of known urease inhibitors with a high-throughput (HT) approach. Interestingly, we found that well-known urease inhibitors such as boric acid and fluoride (Figure 4) were unable to exert their inhibition effect on the cytoplasmatic urease, probably because of their incapability to penetrate into the bacteria. A known competitive inhibitor such acetohydroxamic acid (AHA), which has some known applications in therapy, demonstrated a moderate decrease of in-cell enzymatic activity only at high concentrations and at lower substrate concentrations (Figure 5), indicating the preservation of the competitive inhibition mechanism, as well as revealing its limited bioavailability. On the other hand, the efficacy of the competitive and slow-binding inhibitor N-(n-butyl)-thiophosphoric triamide (NBPT, Figure 6) and of the uncompetitive inhibitor 1,4-benzoquinone (BQ, Figure 7) proved to be conserved in cell at the concentrations effective *in vitro*. Notably, this means that BQ and NBPT (and/or its hydrolyzed derivative NBPD) are able to penetrate the cytoplasmic membrane and carry out urease inhibition within the cell. This is consistent with recent reports of NBPT being able to decrease the growth of ureolytic bacteria such as *S. pasteurii* [43]as well as with older evidence for NBPT toxicity for plants [44–50]. Therefore, the use of the well-characterized Gram-negative *E. coli* as a model for drug administration to the pathogenic bacterium *H. pylori*, whose slow growth and absence of standard genetic tools hampers the implementation of HT assays, proved to be a robust and cost-effective prototype to directly evaluate membrane permeability and urease inhibition of a large number of compounds.

An alternative route to inhibit urease is to prevent the Ni(II) ions insertion into the active site, blocking the PPIs between the urease metallo-chaperones. This is a strategy yet unexplored

that might bring innovative solutions. Within this type of approach, a bismuth-based drug, a known treatment against *H. pylori* that impacts on the activity of urease, was recently found to impair the function of the accessory protein UreG, and thus the urease maturation, resulting in the attenuated virulence of the pathogen [51].

Although the identification of selective, potent and effective inhibitors for PPIs is more difficult than for traditional targets, largely because of the extended nature of the PPI interfaces, remarkable progresses have been made in discovery, characterization and development of small molecules (SMs) as PPI inhibitors in the recent years[52]. These successes are due to the finding of the importance for the interaction of a limited number of “hot spot” residues at the protein interfaces, often included in a short peptide, estimated to contribute most significantly to the binding energy between the protein partners[53]. The ability to localize these “hot segments” in protein-protein interfaces has been crucial for providing an optimal lead for drug design, because these peptides can compete with the proteins from which they were derived, hindering the binding to the cognate interactors.

Based on the structural information available and using the Peptiderive protocol [37], we could identify, at the dimer interface of the $UreF_2$-$UreD_2$ complex, a peptide from the C-termini of UreF largely involved in the interaction with UreD, thus possibly interfering, if expressed alone, with this PPI. This region is likely affected by intrinsic disorder in the isolated protein, as revealed by its proteolytic degradation when UreF is expressed in the absence of its partner, while it undergoes folding into an $\alpha$-helical structure upon interaction with UreD. Typically, PPIs that require folding upon binding are more easily blocked by SMs, and thus this interface represents an ideal target for drug discovery[54,55]. In addition, this part of the complex contains a Ni(II) binding site, likely being part of the route for Ni(II) delivery into

urease [18,56,57]. Disrupting such interaction interface therefore provides a promising strategy to prevent Ni(II) delivery and consequent urease maturation.

Using the genetic tools of the *E. coli* model, we developed a two-plasmids system to prove the essentiality of this segment for the formation of a productive PPI, by C-terminal truncation of the *ureF* gene on the urease operon and subsequent complementation with the wild type gene (Figure 8). These results showed that this interface represents a promising region to be targeted with a SM that mimics the UreF C-terminal peptide sequence.

Oligopeptides are often used for interfering with protein interaction sites, as their modular nature, the low toxicity, and the possibility to screen a large number of molecules through combinatorial approaches, render these chemical species a favorable solution. However, screening and optimizing peptide sequences has been challenging due to the difficulty of these molecules to penetrate the cellular membrane. To explore the ability of the identified peptide to inhibit urease activity in the intracellular environment, we applied the newly developed two-plasmid system to co-express, together with the wild type urease enzyme, the candidate sequence. We found that induction of peptide expression significantly reduced urease activity in cell – while no inhibition was observed in the absence of the arabinose inducer - therefore proving that the identified sequence represents a promising lead peptide structure (Figure 8).

The two-plasmid system described here has the potential to significantly facilitate the screening process of interfering peptides, as the candidates can be generated intracellularly and, starting from the C-terminal segment of UreF, undergo mutagenesis and in-cell testing for the phenotype-specific inhibition using the in-cell assay described above. This would avoid the need of expensive peptide synthesis, as well as of protein and peptide purification. This

strategy, based on directed evolution to dissect PPIs, is emerging as a way to generate variants with increasing affinity for the protein interfaces [58]. In addition, the possibility of studying the biological role of PPIs in a native cellular environment is fundamental to avoid artifacts and drive data interpretations. The identified interfering sequence can be the basis for future work of drug design of peptidomimetics and SMs with higher pharmacological potential.

In conclusion, this work describes a robust and reliable method to evaluate, directly in the cell, the drug potential of known *H. pylori* urease inhibitors with diverse action modes, such as competitive, uncompetitive or slow-binding, as well as the role of interfering peptides in interrupting the PPI network leading to urease maturation. The developed system renders thus feasible the concomitant screening of a large number of drug candidates that interfere with the enzyme activity both at the level of the enzyme catalysis and maturation. Among the twelve most important bacteria listed in 2017 by WHO as a global threat because of the emerging development of antimicrobial resistance (https://goo.gl/vLRURp) [7], ten produce urease, the activity of which is demonstrated as a pathogenic factor for some of them, beside *H. pylori*: for example, *Pseudomonas aeruginosa* and *Staphylococcus aureus* urease activity determines biofilm formation [59,60], for *P. mirabilis* [61], *Staphylococcus saprophyticus* [62] and *Ureaplasma urealyticum* [63] urease activity plays a central role for infection and urea stones formation in the urinary tract. Inhibition of this enzyme has therefore the potential of being a global antibacterial strategy for a large number of infections. This work paves the way for the development and evolution of new drug candidates that can be applied, in the future, also to other bacterial targets.

## 5. Acknowledgements

This work was supported by the Department of Pharmacy and Biotechnology of the University of Bologna through funds for fundamental research (to BZ, AD and SC) and grant FARB Project RFBO120249 of the Department of Pharmacy and Biotechnology. The authors also thank Dr Luca Mazzei for useful discussions on the experimental set up of the in cell assays.

## 6. References


[1] T.L. Testerman, J. Morris, Beyond the stomach: an updated view of Helicobacter pylori pathogenesis, diagnosis, and treatment., World J. Gastroenterol. 20 (2014) 12781–808. doi:10.3748/wjg.v20.i36.12781.

[2] IARC, Schistosomes, liver flukes and Helicobacter pylori., 1994. doi:PMID 7715068.

[3] IARC, Helicobacter pylori, in: IARC Monogr. – 100B, Lyon - France, 2012: pp. 385–435. http://monographs.iarc.fr/ENG/Monographs/vol100B/mono100B-15.pdf (accessed April 28, 2018).

[4] IARC, Helicobacter pylori Eradication as a Strategy for Preventing Gastric Cancer, (2014). http://www.iarc.fr/en/publications/pdfs-online/wrk/wrk8/index.php (accessed April 4, 2018).

[5] A. Stathis, F. Bertoni, E. Zucca, Treatment of gastric marginal zone lymphoma of MALT type, Expert Opin. Pharmacother. 11 (2010) 2141–2152. doi:10.1517/14656566.2010.497141.

[6] N.J. Talley, K.M. Fock, P. Moayyedi, Gastric Cancer Consensus conference recommends Helicobacter pylori screening and treatment in asymptomatic persons from high-risk populations to prevent gastric cancer., in: Am. J. Gastroenterol., 2008: pp. 510–514. doi:10.1111/j.1572-0241.2008.01819.x.

[7] W.H.O. WHO, Global priority list of antibiotic-resistant bacteria to guide research, discovery, and development of new antibiotics, n.d.

[8] B. Zambelli, F. Musiani, S. Benini, S. Ciurli, Chemistry of Ni2+ in urease: Sensing, trafficking, and catalysis, Acc. Chem. Res. 44 (2011) 520–530. doi:10.1021/ar200041k.

[9] B. Zambelli, S. Ciurli, Nickel and human health, Met. Ions Life Sci. 13 (2013) 321–357.

doi:10.1007/978-94-007-7500-8-10.

[10] K.A. Eaton, C.L. Brooks, D.R. Morgan, S. Krakowka, Essential Role of Urease in Pathogenesis of Gastritis Induced by *Helicobacter pylori* in Gnotobiotic Piglets, Infect. Immun. 59 (1991) 2470–2475.

[11] K.A. Eaton, S. Krakowka, Effect of gastric pH on urease-dependent colonization of gnotobiotic piglets by Helicobacter pylori, Infect. Immun. 62 (1994) 3604–3607.

[12] M. Campanale, E. Nucera, V. Ojetti, V. Cesario, T.A. Di Rienzo, G. D'Angelo, S. Pecere, F. Barbaro, G. Gigante, T. De Pasquale, A. Rizzi, G. Cammarota, D. Schiavino, F. Franceschi, A. Gasbarrini, Nickel free-diet enhances the Helicobacter pylori eradication rate: A pilot study, Dig. Dis. Sci. 59 (2014) 1851–1855. http://eutils.ncbi.nlm.nih.gov/entrez/eutils/elink.fcgi?dbfrom=pubmed&id=24595654&retmode=ref&cmd=prlinks.

[13] M.J. Maroney, S. Ciurli, Nonredox nickel enzymes., Chem. Rev. 114 (2014) 4206–28. doi:10.1021/cr4004488.

[14] A. Merloni, O. Dobrovolska, B. Zambelli, F. Agostini, M. Bazzani, F. Musiani, S. Ciurli, Molecular landscape of the interaction between the urease accessory proteins UreE and UreG, Biochim. Biophys. Acta - Proteins Proteomics. 1844 (2014) 1662–1674. doi:10.1016/j.bbapap.2014.06.016.

[15] B. Zambelli, P. Turano, F. Musiani, P. Neyroz, S. Ciurli, Zn2+-linked dimerization of UreG from Helicobacter pylori, a chaperone involved in nickel trafficking and urease activation, Proteins Struct. Funct. Bioinforma. 74 (2009) 222–239. doi:10.1002/prot.22205.

[16] M. Bellucci, B. Zambelli, F. Musiani, P. Turano, S. Ciurli, *Helicobacter pylori* UreE, a urease accessory protein: specific $Ni^{2+}$ - and $Zn^{2+}$ -binding properties and interaction

with its cognate UreG, Biochem. J. 422 (2009) 91–100. doi:10.1042/BJ20090434.

[17] Y.H. Fong, H.C. Wong, M.H. Yuen, P.H. Lau, Y.W. Chen, K.-B. Wong, Structure of UreG/UreF/UreH complex reveals how urease accessory proteins facilitate maturation of Helicobacter pylori urease., PLoS Biol. 11 (2013) e1001678. doi:10.1371/journal.pbio.1001678.

[18] B. Zambelli, A. Berardi, V. Martin-Diaconescu, L. Mazzei, F. Musiani, M.J. Maroney, S. Ciurli, Nickel binding properties of Helicobacter pylori UreF, an accessory protein in the nickel-based activation of urease, J. Biol. Inorg. Chem. 19 (2014) 319–334. doi:10.1007/s00775-013-1068-3.

[19] J.H. Urban, J. Vogel, Translational control and target recognition by Escherichia coli small RNAs in vivo, Nucleic Acids Res. 35 (2007) 1018–1037. doi:10.1093/nar/gkl1040.

[20] J. Bogomolovas, B. Simon, M. Sattler, G. Stier, Screening of fusion partners for high yield expression and purification of bioactive viscotoxins., Protein Expr. Purif. 64 (2009) 16–23. doi:10.1016/j.pep.2008.10.003.

[21] N. Amar, A. Peretz, Y. Gerchman, A cheap, simple high throughput method for screening native Helicobacter pylori urease inhibitors using a recombinant Escherichia coli, its validation and demonstration of Pistacia atlantica methanolic extract effectivity and specificity., J. Microbiol. Methods. 133 (2017) 40–45. http://linkinghub.elsevier.com/retrieve/pii/S0167701216303438.

[22] M.J. Todd, J. Gomez, Enzyme kinetics determined using calorimetry: A general assay for enzyme activity?, Anal. Biochem. 296 (2001) 179–187. doi:10.1006/abio.2001.5218.

[23] S. Benini, M. Cianci, L. Mazzei, S. Ciurli, Fluoride inhibition of Sporosarcina pasteurii urease: structure and thermodynamics., J. Biol. Inorg. Chem. 19 (2014) 1243–61. doi:10.1007/s00775-014-1182-x.

[24] S. Benini, W.R. Rypniewski, K.S. Wilson, S. Mangani, S. Ciurli, Molecular details of urease inhibition by boric acid: insights into the catalytic mechanism., J. Am. Chem. Soc. 126 (2004) 3714–5. doi:10.1021/ja049618p.

[25] B. Krajewska, Ureases I. Functional, catalytic and kinetic properties: A review, J. Mol. Catal. B Enzym. 59 (2009) 9–21. doi:10.1016/j.molcatb.2009.01.003.

[26] M.A. Pearson, L.O. Michel, R.P. Hausinger, P.A. Karplus, Structures of Cys319 variants and acetohydroxamate-inhibited Klebsiella aerogenes urease, Biochemistry. 36 (1997) 8164–8172. doi:10.1021/bi970514j.

[27] S. Benini, W.R. Rypniewski, K.S. Wilson, S. Miletti, S. Ciurli, S. Mangani, The complex of Bacillus pasteurii urease with acetohydroxamate anion from X-ray data at 1.55 A resolution., J. Biol. Inorg. Chem. 5 (2000) 110–8. doi:10.1007/s007750050014.

[28] N. Ha, S. Oh, J.Y. Sung, K.A. Cha, M.H. Lee, B. Oh, Supramolecular assembly and acid resistance of Helicobacter pylori urease, Nat. Struct. Biol. 8 (2001) 505–509. doi:10.1038/88563.

[29] K. Phillips, D.J. Munster, R. a Allardyce, P.F. Bagshaw, Antibacterial action of the urease inhibitor acetohydroxamic acid on Helicobacter pylori., J. Clin. Pathol. 46 (1993) 372–373. doi:10.1136/jcp.46.4.372.

[30] D.P. Griffith, M.J. Gleeson, H. Lee, R. Longuet, E. Deman, N. Earle, Randomized, double-blind trial of Lithostat (acetohydroxamic acid) in the palliative treatment of infection-induced urinary calculi., Eur. Urol. 20 (1991) 243–247.

[31] N.C. Bailie, C.A. Osborne, J.R. Leininger, T.F. Fletcher, S.D. Johnston, P.N. Ogburn, D.P. Griffith, Teratogenic effect of acetohydroxamic acid in clinically normal Beagles, Am. J. Vet. Res. 47 (1986) 2604–2611.

[32] A.J. Pope, C.D.N. Toseland, B. Rushant, S. Richardson, M. Mcvey, J. Hills, Effect of

potent urease inhibitor, fluorofamide, on Helicobacter sp. in vivo and in vitro, Dig. Dis. Sci. 43 (1998) 109–119. doi:10.1023/A:1018884322973.

[33] K. Macegoniuk, E. Grela, M. Biernat, M. Psurski, G. Gościniak, A. Dziełak, A. Mucha, J. Wietrzyk, Ł. Berlicki, A. Grabowiecka, Aminophosphinates against Helicobacter pylori ureolysis-Biochemical and whole-cell inhibition characteristics., PLoS One. 12 (2017) e0182437. http://journals.plos.org/plosone/article?id=10.1371/journal.pone.0182437.

[34] P. Kosikowska, Ł. Berlicki, Urease inhibitors as potential drugs for gastric and urinary tract infections: a patent review., Expert Opin. Ther. Pat. 21 (2011) 945–957. doi:10.1517/13543776.2011.574615.

[35] L. Mazzei, M. Cianci, U. Contaldo, F. Musiani, S. Ciurli, Urease inhibition in the presence of N-(n-butyl)thiophosphoric triamide, a suicide substrate: structure and kinetics., Biochemistry. 56 (2017) 5391–5404. doi:10.1021/acs.biochem.7b00750.

[36] L. Mazzei, M. Cianci, F. Musiani, S. Ciurli, Inactivation of urease by 1,4-benzoquinone: chemistry at the protein surface, Dalt. Trans. 45 (2016) 5455–5459. doi:10.1039/C6DT00652C.

[37] Y. Sedan, O. Marcu, S. Lyskov, O. Schueler-Furman, Peptiderive server: derive peptide inhibitors from protein-protein interactions, Nucleic Acids Res. 44 (2016) W536–W541. doi:10.1093/nar/gkw385.

[38] Y.H. Fong, H.C. Wong, C.P. Chuck, Y.W. Chen, H. Sun, K.B. Wong, Assembly of preactivation complex for urease maturation in Helicobacter pylori: Crystal structure of UreF-UreH protein complex, J. Biol. Chem. 286 (2011) 43241–43249. doi:10.1074/jbc.M111.296830.

[39] R. Lam, V. Romanov, K. Johns, K.P. Battaile, J. Wu-Brown, J.L. Guthrie, R.P. Hausinger, E.F. Pai, N.Y. Chirgadze, Crystal structure of a truncated urease accessory

protein UreF from Helicobacter pylori, Proteins Struct. Funct. Bioinforma. 78 (2010) 2839–2848. doi:10.1002/prot.22802.

[40] P. Zhou, G. Wagner, Overcoming the solubility limit with solubility-enhancement tags: successful applications in biomolecular NMR studies., J. Biomol. NMR. 46 (2010) 23–31. doi:10.1007/s10858-009-9371-6.

[41] C. Follmer, Ureases as a target for the treatment of gastric and urinary infections, J. Clin. Pathol. 63 (2010) 424–430. doi:10.1136/jcp.2009.072595.

[42] K. Macegoniuk, E. Grela, J. Palus, E. Rudzińska-Szostak, A. Grabowiecka, M. Biernat, Ł. Berlicki, 1,2-Benzisoselenazol-3(2H)-one Derivatives As a New Class of Bacterial Urease Inhibitors., J. Med. Chem. 59 (2016) 8125–8133. http://eutils.ncbi.nlm.nih.gov/entrez/eutils/elink.fcgi?dbfrom=pubmed&id=27524377&retmode=ref&cmd=prlinks.

[43] L. Mazzei, V. Broll, S. Ciurli, An Evaluation of Maleic-Itaconic Copolymers as Urease Inhibitors, Soil Sci. Soc. Am. J. (2018). doi:10.2136/sssaj2017.09.0323.

[44] J.M. Bremner, Recent research on problems in the use of urea as a nitrogen fertilizer, Fertil. Res. 42 (1995) 321–329. doi:10.1007/BF00750524.

[45] M.J. Krogmeier, G.W. McCarty, J.M. Bremner, Potential phytotoxicity associated with the use of soil urease inhibitors, Proc. Natl. Acad. Sci. 86 (1989) 1110–1112. doi:10.1073/pnas.86.4.1110.

[46] C.J. Watson, H. Miller, Short-term effects of urea amended with the urease inhibitor N-(n-butyl) thiophosphoric triamide on perennial ryegrass, Plant Soil. 184 (1996) 33–45. doi:10.1007/BF00029272.

[47] E. Artola, S. Cruchaga, I. Ariz, J.F. Moran, M. Garnica, F. Houdusse, J.M.G. Mina, I. Irigoyen, B. Lasa, P.M. Aparicio-Tejo, Effect of N-(n-butyl) thiophosphoric triamide on

urea metabolism and the assimilation of ammonium by Triticum aestivum L, Plant Growth Regul. 63 (2011) 73–79. doi:10.1007/s10725-010-9513-6.

[48] S. Cruchaga, E. Artola, B. Lasa, I. Ariz, I. Irigoyen, J.F. Moran, P.M. Aparicio-Tejo, Short term physiological implications of NBPT application on the N metabolism of Pisum sativum and Spinacea oleracea, J. Plant Physiol. 168 (2011) 329–336. doi:10.1016/j.jplph.2010.07.024.

[49] L. Zanin, N. Tomasi, A. Zamboni, Z. Varanini, R. Pinton, The Urease Inhibitor NBPT Negatively Affects DUR3-mediated Uptake and Assimilation of Urea in Maize Roots, Front. Plant Sci. 6 (2015). doi:10.3389/fpls.2015.01007.

[50] L. Zanin, S. Venuti, N. Tomasi, A. Zamboni, R.M. De Brito Francisco, Z. Varanini, R. Pinton, Short-Term Treatment with the Urease Inhibitor N-(n-Butyl) Thiophosphoric Triamide (NBPT) Alters Urea Assimilation and Modulates Transcriptional Profiles of Genes Involved in Primary and Secondary Metabolism in Maize Seedlings, Front. Plant Sci. 7 (2016). doi:10.3389/fpls.2016.00845.

[51] X. Yang, M. Koohi-Moghadam, R. Wang, Y.Y. Chang, P.C.Y. Woo, J. Wang, H. Li, H. Sun, Metallochaperone UreG serves as a new target for design of urease inhibitor: A novel strategy for development of antimicrobials, PLoS Biol. 16 (2018). doi:10.1371/journal.pbio.2003887.

[52] C. Sheng, G. Dong, Z. Miao, W. Zhang, W. Wang, State-of-the-art strategies for targeting protein-protein interactions by small-molecule inhibitors., Chem. Soc. Rev. 44 (2015) 8238–8259. http://xlink.rsc.org/?DOI=C5CS00252D.

[53] N. London, B. Raveh, D. Movshovitz-Attias, O. Schueler-Furman, Can self-inhibitory peptides be derived from the interfaces of globular protein-protein interactions?, Proteins Struct. Funct. Bioinforma. 78 (2010) 3140–3149. doi:10.1002/prot.22785.

[54] G.T. Heller, F.A. Aprile, M. Vendruscolo, Methods of probing the interactions between small molecules and disordered proteins., Cell. Mol. Life Sci. 74 (2017) 3225–3243. http://link.springer.com/10.1007/s00018-017-2563-4.

[55] V.N. Uversky, Intrinsic disorder-based protein interactions and their modulators., Curr. Pharm. Des. 19 (2013) 4191–4213. http://eutils.ncbi.nlm.nih.gov/entrez/eutils/elink.fcgi?dbfrom=pubmed&id=23170892&retmode=ref&cmd=prlinks.

[56] F. Biagi, F. Musiani, S. Ciurli, Structure of the UreD-UreF-UreG-UreE complex in Helicobacter pylori: A model study, J. Biol. Inorg. Chem. 18 (2013) 571–577. doi:10.1007/s00775-013-1002-8.

[57] F. Musiani, D. Gioia, M. Masetti, F. Falchi, A. Cavalli, M. Recanatini, S. Ciurli, Protein Tunnels: The Case of Urease Accessory Proteins, J. Chem. Theory Comput. 13 (2017) 2322–2331. doi:10.1021/acs.jctc.7b00042.

[58] D.A. Bonsor, E.J. Sundberg, Dissecting protein-protein interactions using directed evolution, Biochemistry. 50 (2011) 2394–2402. http://pubs.acs.org/doi/abs/10.1021/bi102019c.

[59] K.E. Beenken, P.M. Dunman, F. McAleese, D. Macapagal, E. Murphy, S.J. Projan, J.S. Blevins, M.S. Smeltzer, Global gene expression in Staphylococcus aureus biofilms., J Bacteriol. 186 (2004) 4665–4684. http://eutils.ncbi.nlm.nih.gov/entrez/eutils/elink.fcgi?dbfrom=pubmed&id=15231800&retmode=ref&cmd=prlinks.

[60] M. Müsken, S. Di Fiore, A. Dötsch, R. Fischer, S. Häussler, Genetic determinants of Pseudomonas aeruginosa biofilm establishment., Microbiol. (Reading, Engl). 156 (2010) 431–441.

http://eutils.ncbi.nlm.nih.gov/entrez/eutils/elink.fcgi?dbfrom=pubmed&id=19850623&retmode=ref&cmd=prlinks.

[61] B.D. Jones, C. V. Lockatell, D.E. Johnson, J.W. Warren, H.L.T. Mobley, Construction of a urease-negative mutant of Proteus mirabilis: Analysis of virulence in a mouse model of ascending urinary tract infection, Infect. Immun. 58 (1990) 1120–1123.

[62] S. Gatermann, R. Marre, Cloning and expression of Staphylococcus saprophyticus urease gene sequences in Staphylococcus carnosus and contribution of the enzyme to virulence, Infect. Immun. 57 (1989) 2998–3002.

[63] J. V. Ligon, G.E. Kenny, Virulence of ureaplasmal urease for mice, Infect. Immun. 59 (1991) 1170–1171.